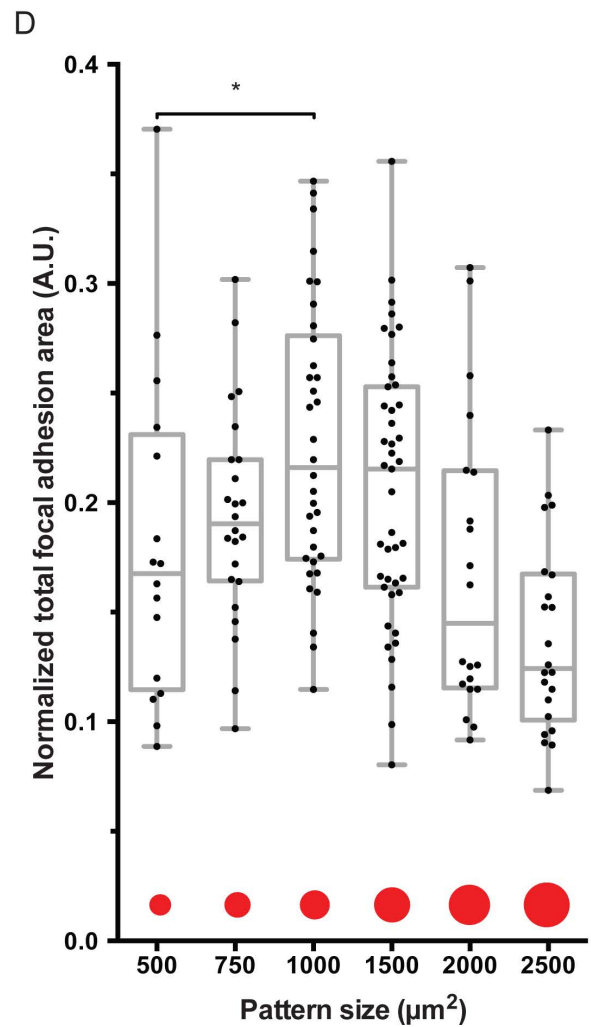
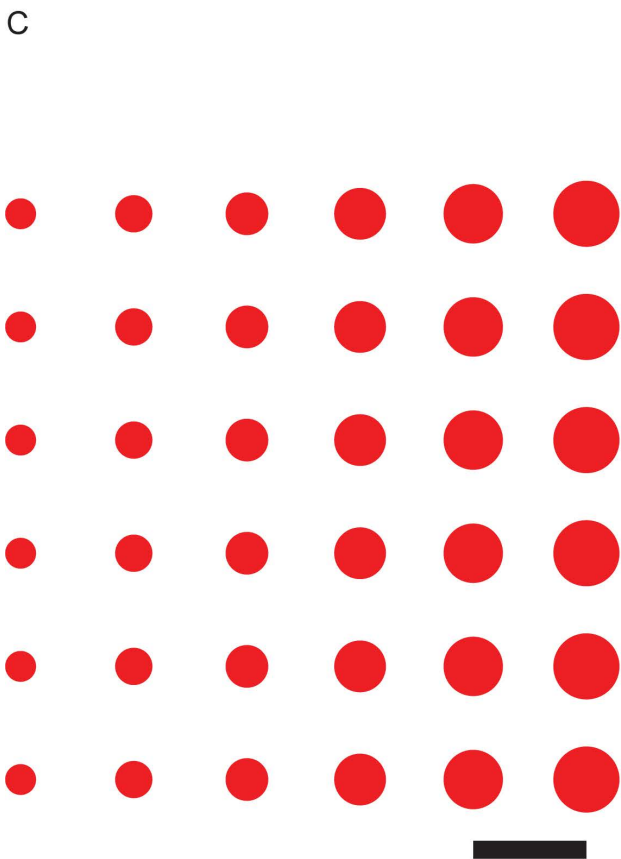
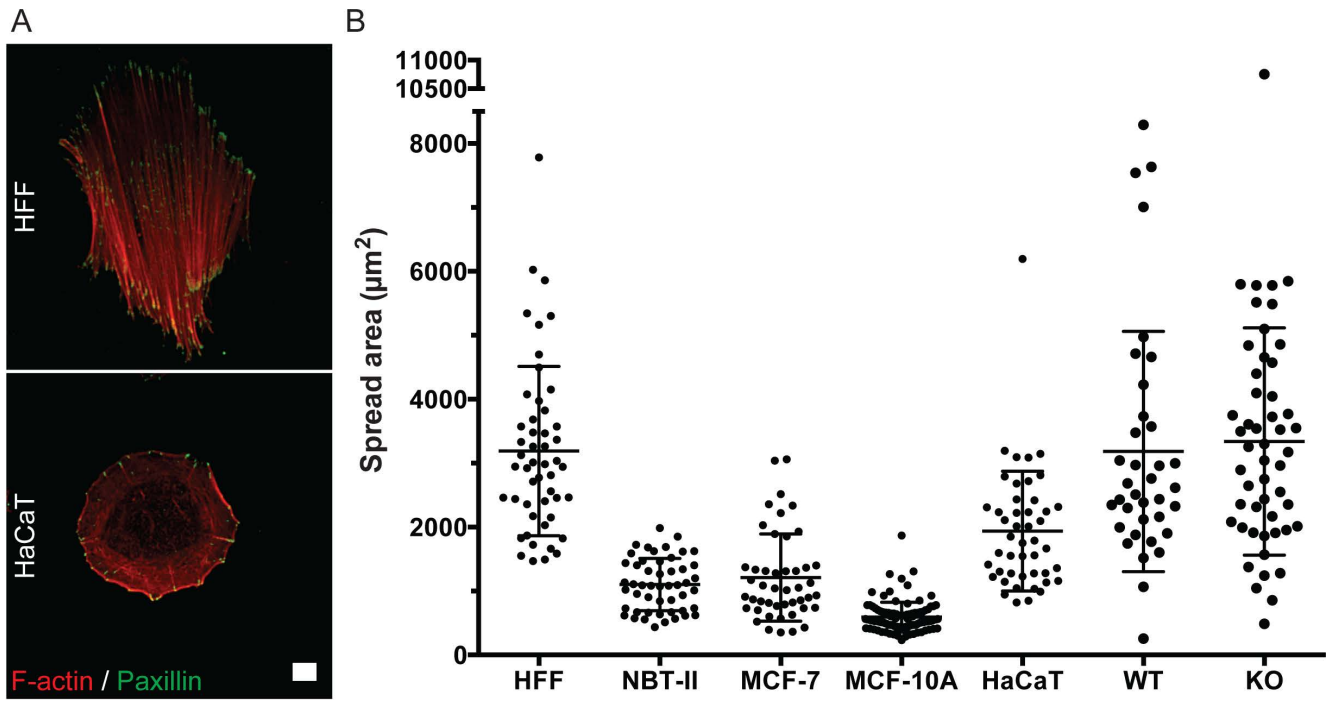


### Supplemental Figures



**Figure S1: Cell morphology and spread area variation between epithelial cell lines and fibroblasts**

**A)** Representative images showing focal adhesion (paxillin immunostaining) and F-actin (phalloidin staining) distribution in HFF and HaCaT fixed 24 h after seeding on planar fibronectin-coated surfaces. Scale bar: 10  $\mu\text{m}$ .

**B)** Scatter dot plot with Mean  $\pm$  Standard Deviation showing cell spread area of different cell lines on planar protein-coated surfaces. HFF, NBT-II and HaCaT were fixed and stained with phalloidin 24 h after seeding on planar fibronectin-coated surfaces. Wild-type (WT) and Knockout (KO) murine keratinocytes were fixed and stained with phalloidin 22 h after seeding on planar collagen-coated surfaces. MCF-7 and MCF-10A were fixed and stained with phalloidin 18 h after seeding on planar collagen-coated surfaces.

**C)** Schematic showing pattern consisting of six different sizes of circular islands that was used for protein patterning. Scale bar: 50  $\mu\text{m}$ .

**D)** Box and whiskers plot showing the total focal adhesion area in cells imaged under conditions of Fig. 1E normalized by projected cell area. Mann-Whitney tests were used to assess significance between the normalized total focal adhesion areas in pairs of island sizes;  $*P < 0.05$ . The box represents the 25–75th percentiles, and the median is indicated. The whiskers show the complete range from minimum to maximum values. Points superimposed on the graph show all values.

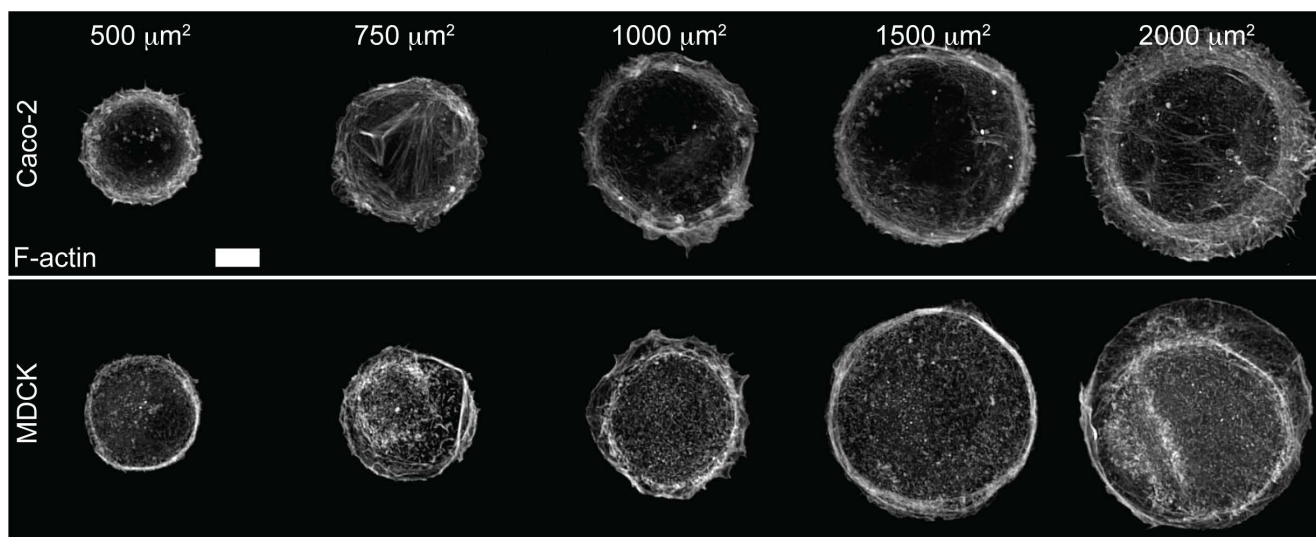


**Figure S2: Actin cytoskeleton development in non-keratinocyte epithelial cell lines**

Representative images showing actin cytoskeleton organization (phalloidin stained) in Caco-2 and MDCK fixed 20-24 h after seeding on collagen-coated islands of different sizes (500, 750, 1000, 1500, 2000 and 2500  $\mu\text{m}^2$ ). Scale bar: 10  $\mu\text{m}$ .

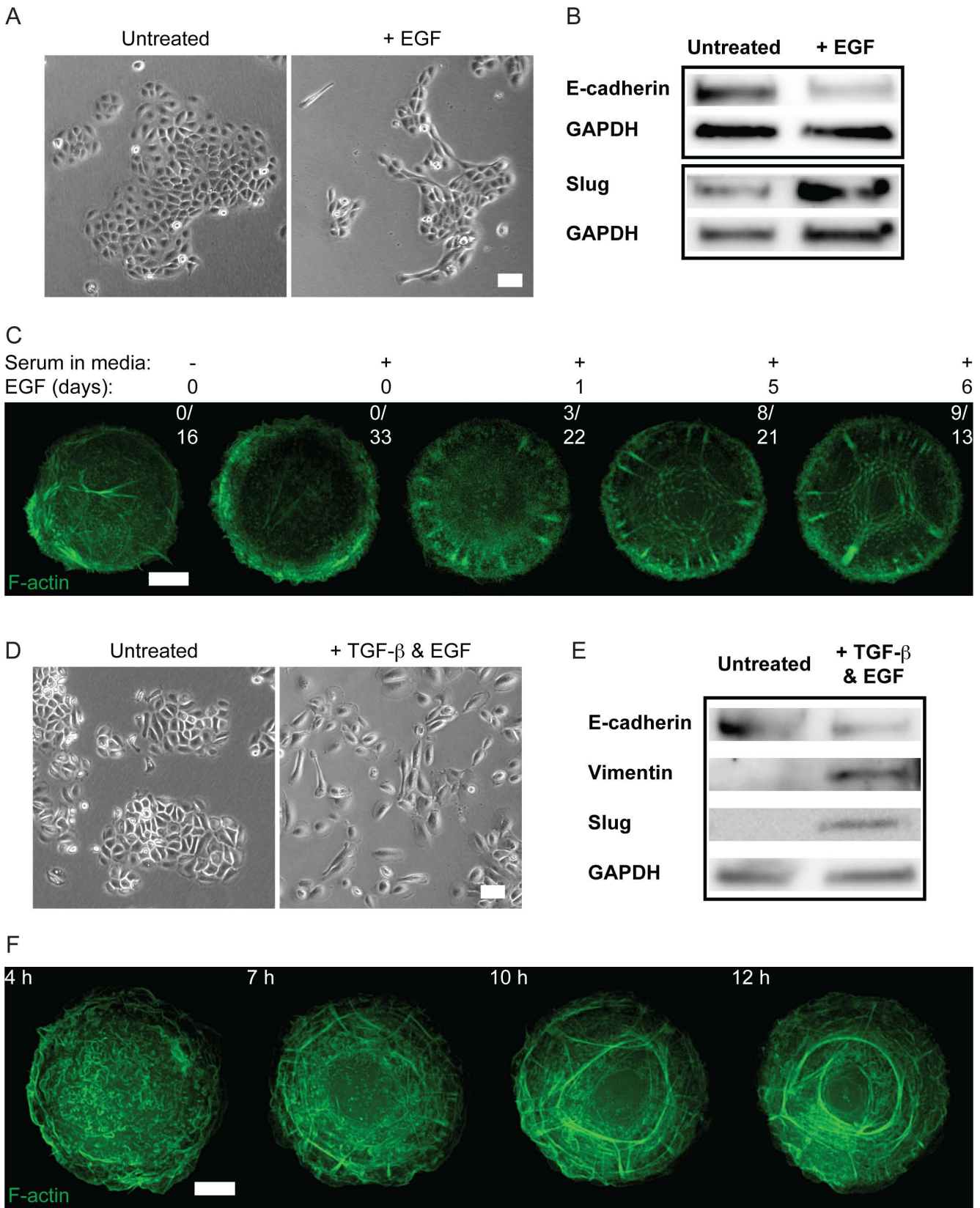


**Figure S3: Actin cytoskeleton development during epithelial-mesenchymal transition in rat bladder carcinoma cells and human keratinocytes**

**A)** Representative brightfield images of NBT-II in standard culture after cells were left untreated (Untreated, left panel) or treated with 100 ng ml<sup>-1</sup> EGF for 3 days (+EGF, right panel). Scale bar: 100 μm.

**B)** Western blot images showing protein expression levels of E-cadherin, Slug and GAPDH in total protein lysates taken from NBT-II cells without (Untreated) or with (+EGF) 100 ng ml<sup>-1</sup> EGF treatment for 3 days.

**C)** Representative frames of actin cytoskeleton organization in NBT-II cultured in serum free or serum containing media with or without 100 ng ml<sup>-1</sup> EGF pre-treatment (in days). Cells were transfected with Lifeact-GFP one day before replating and imaging overnight on 1200 μm<sup>2</sup> fibronectin-coated islands. Fractions of cells able to develop radial fibres (over total number of imaged cells) are shown in the top right corner of each frame representing a treatment condition. Scale bar: 10 μm.

**D)** Representative brightfield images of HaCaT in standard culture after cells were left untreated (left panel), or, treated with EGF and TGF-β for 3 days (as described in Materials and methods, right panel). Scale bar: 100 μm.

**E)** Western blot images showing protein expression levels of E-cadherin, vimentin, slug and GAPDH in total protein lysates taken from HaCaT cells without (Untreated) or with (+TGF-β & EGF) growth factor treatment for 5 days.

**F)** Representative time-lapse series of actin pattern development in HaCaT cells replated on 1800 μm<sup>2</sup> fibronectin-coated islands after 4 days of growth factor treatment. Cells were transfected with Lifeact-GFP one day before replating and imaging overnight. Time in hours after seeding is indicated in upper left corner of each frame. Scale bar: 10 μm.



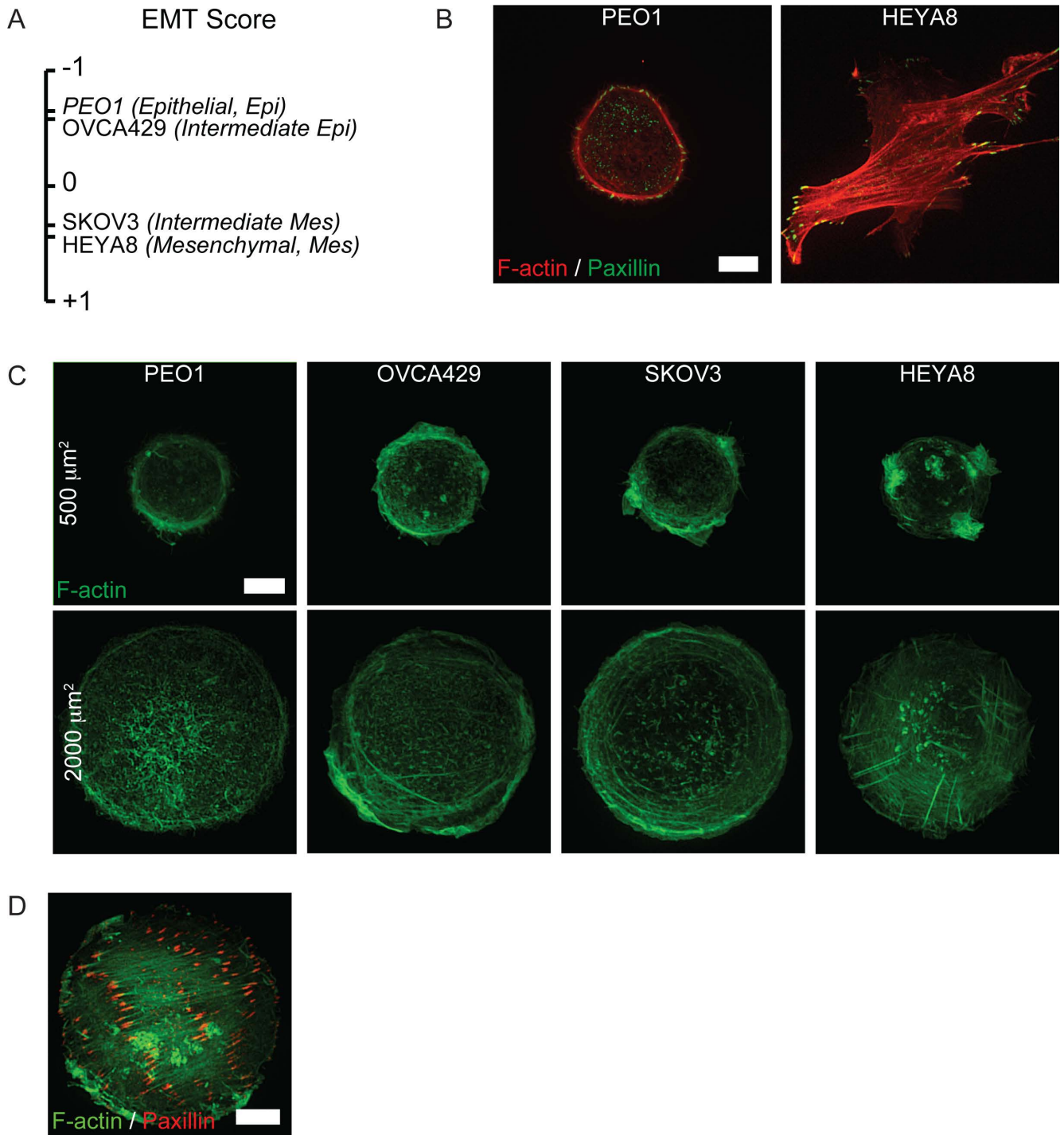


**Figure S4: Actin cytoskeleton self-organization in ovarian cancer cell lines**

**A)** A selection of ovarian cancer cell lines (PEO1, OVCA429, SKOV3 and HEYA8) distributed along a scale corresponding to their EMT score (from most epithelial, -1 to most mesenchymal, +1).

**B)** Representative images showing focal adhesion (paxillin immunostaining) and F-actin (phalloidin staining) distribution in epithelial (PEO1) and mesenchymal (HEYA8) ovarian cancer cells fixed 16 h after seeding on planar fibronectin-coated substrates. Scale bar: 10  $\mu\text{m}$ .

**C)** Representative images of ovarian cancer cells with different EMT phenotypes (PEO1, OVCA429, SKOV3 and HEYA8) fixed and stained with phalloidin 16 h after seeding on fibronectin-coated islands of different sizes. Scale bar: 10  $\mu\text{m}$ .

**D)** Representative image showing focal adhesion (paxillin immunostaining) and F-actin (phalloidin staining) distribution in a HEYA8 cell imaged under conditions detailed in **C** that shows the linear actin pattern. Scale bar: 10  $\mu\text{m}$ .

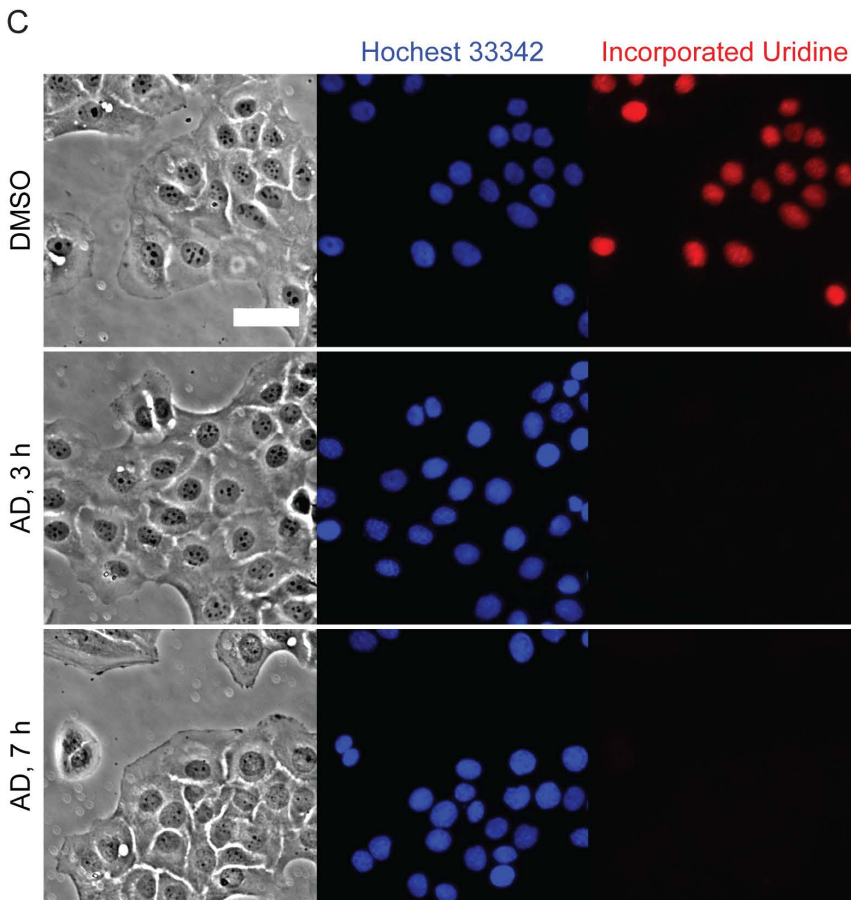
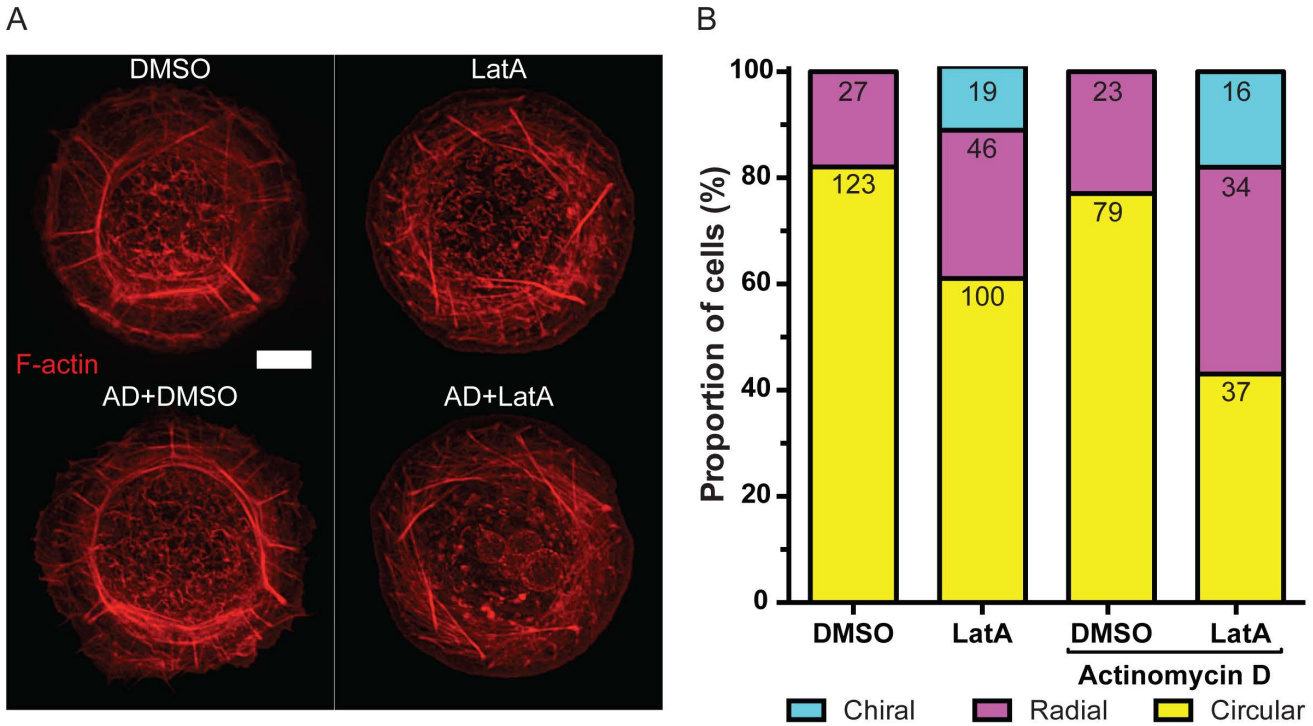




**Figure S5: Chiral actin swirling persists in latrunculin A-treated keratinocytes even when transcriptional changes are suppressed**

**A)** Representative image showing F-actin distribution (phalloidin staining) in keratinocytes that were treated with actinomycin D (AD) or an equivalent volume of DMSO after seeding on 1800  $\mu\text{m}^2$  fibronectin-coated adhesive islands for 2 h and then incubated with actinomycin D during latrunculin A (LatA, 100 nM) treatment before fixing ~7 h after seeding. Scale bar: 10  $\mu\text{m}$ .

**B)** Bar chart showing fractions of cells with actin cytoskeleton demonstrating circular, radial or chiral pattern from cells imaged under conditions of **A**. Numbers of cells displaying each actin pattern are labelled on top of each bar per condition, pooled from 2 independent experiments. Fisher's exact tests were used to assess significance between the fractions of cells displaying each actin pattern in pairs (DMSO vs. AD+DMSO, LatA vs. AD+LatA); no statistically significant differences were calculated.

**C)** Representative images showing brightfield images together with Hoechst 33342 and uridine staining in keratinocytes that were treated with DMSO (upper panel) or 2  $\mu\text{g ml}^{-1}$  actinomycin D for 3 h (middle panel) and 7 h (lower panel) after seeding on fibronectin-coated glass coverslips. Note actinomycin D treated cells lack uridine staining. Scale bar: 50  $\mu\text{m}$ .

**D)** Scatter dot plot with Mean  $\pm$  Standard Deviation showing the incorporation of uridine into newly transcribed RNA, measured from keratinocytes imaged under conditions of **C**.

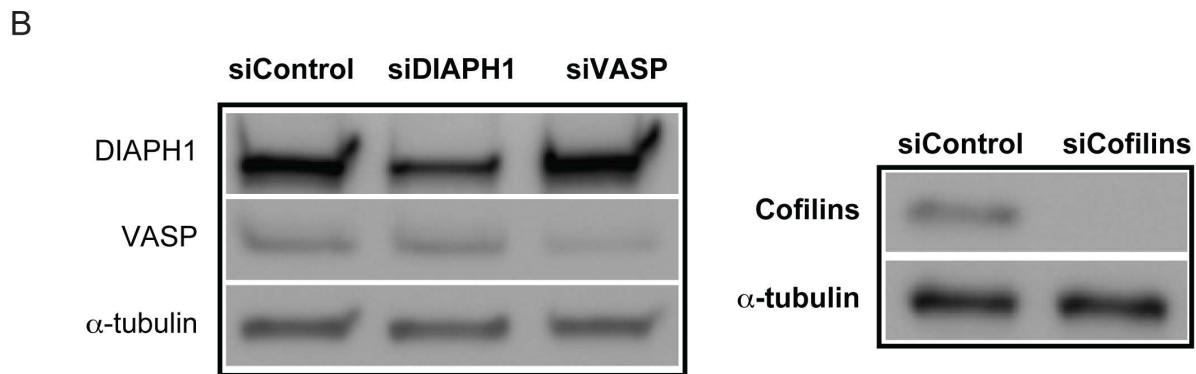
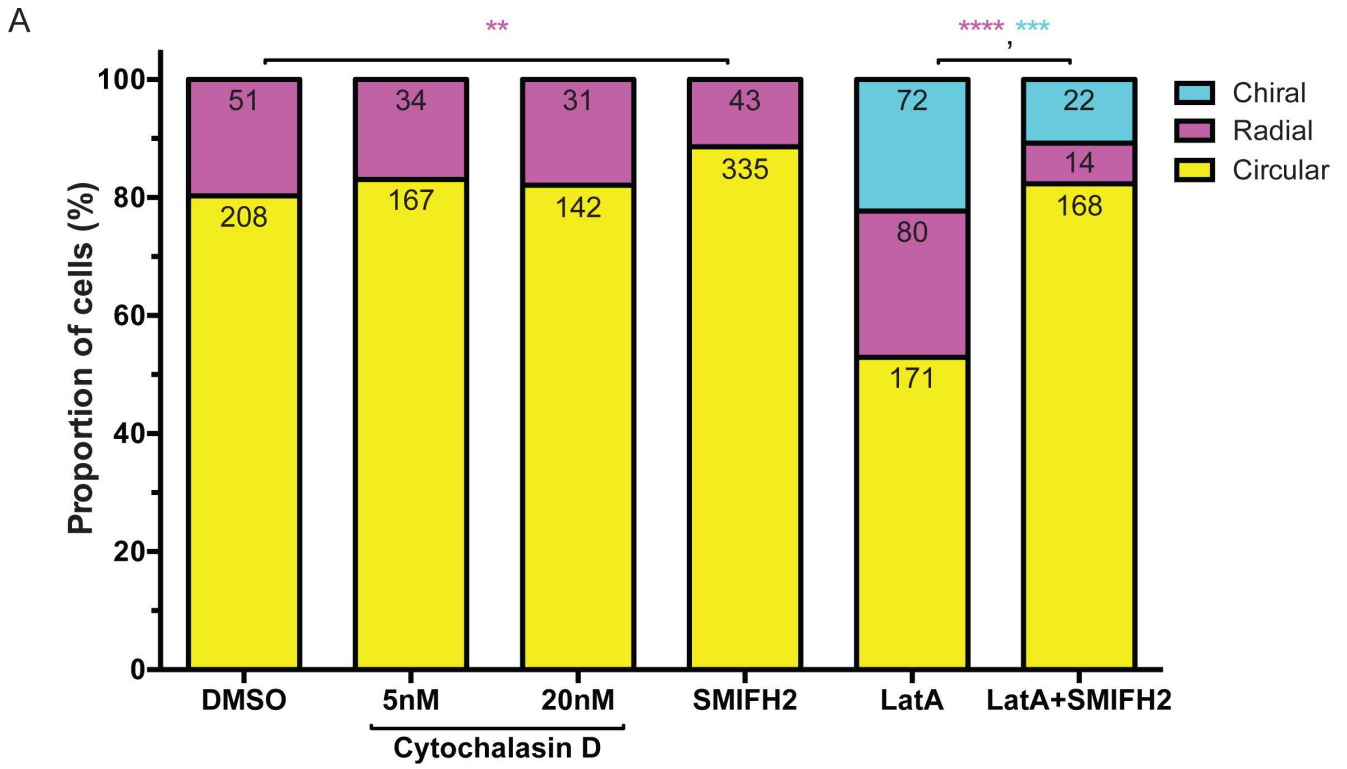


**Figure S6: Effect of inhibitors of actin polymerization on the formation of radial fibres and development of chiral actin patterns in keratinocytes**

**A)** Bar chart showing fractions of cells with actin cytoskeleton demonstrating circular, radial or chiral pattern from HaCaT cells treated with DMSO, 5 nM cytochalasin D, 20 nM cytochalasin D, 15  $\mu$ M SMIFH2, 100 nM latrunculin A (LatA), or 100 nM latrunculin A combined with 15  $\mu$ M SMIFH2 (LatA+SMIFH2) and fixed after overnight seeding on 1800  $\mu$ m<sup>2</sup> fibronectin-coated islands. Numbers of cells displaying each actin pattern are labelled on top of each bar per condition, pooled from 2 independent experiments. Fisher's exact tests were used to assess significance between the fractions of cells displaying radial (magenta asterisk) or chiral (cyan asterisk) actin pattern in pairs (DMSO vs. 5 nM Cytochalasin D, DMSO vs. 20 nM Cytochalasin D, DMSO vs. SMIFH2, LatA vs. LatA+SMIFH2); \* $P$ <0.05, \*\* $P$ <0.01, \*\*\* $P$ <0.001, \*\*\*\* $P$ <0.0001.

**B)** Western blot images showing protein expression levels of DIAPH1, VASP, Cofilins (1 and 2 together) and  $\alpha$ -tubulin in total protein lysates taken from HaCaT cells genetically silenced with Control, DIAPH1, VASP and Cofilins (1 and 2 together) siRNAs.

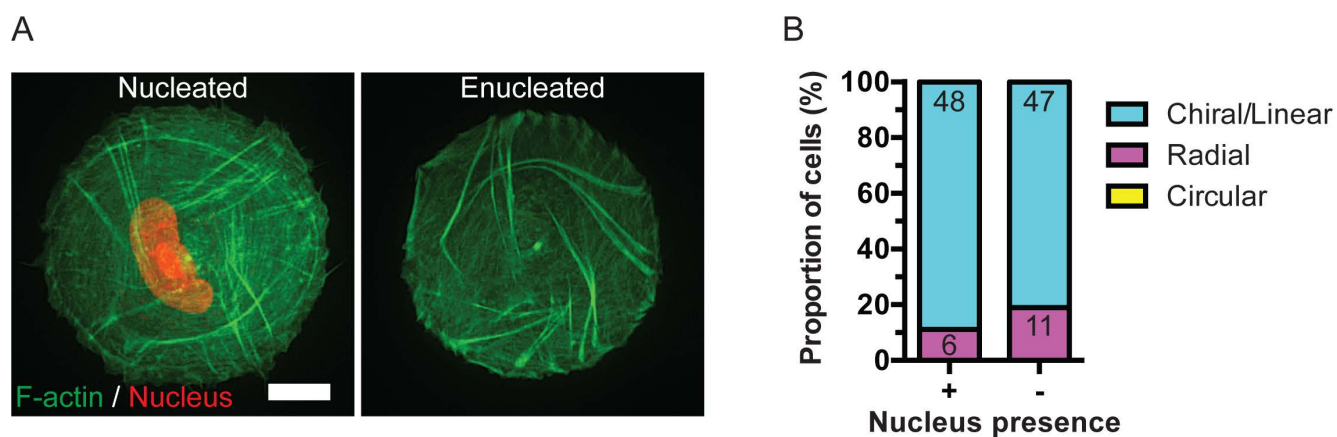


**Figure S7: Chiral actin swirling persists in enucleated fibroblasts**

**A)** Representative frames showing actin cytoskeleton development in nucleated and enucleated (see Materials and methods) HFF cells plated on  $1800 \mu\text{m}^2$  fibronectin-coated adhesive islands, expressing GFP-Lifeact with nucleus marker (BFP-NLS) and additionally stained by Hoechst 33342. Scale bar:  $10 \mu\text{m}$ .

**B)** Bar chart showing fractions of cells with actin cytoskeleton demonstrating circular, radial or chiral pattern from cells imaged under conditions of **A**. Numbers of cells displaying each actin pattern are labelled on top of each bar per condition, pooled from 2 independent experiments. Fisher's exact test was used to assess the significance between the fractions of cells displaying the radial or chiral actin pattern; no statistically significant difference was calculated.

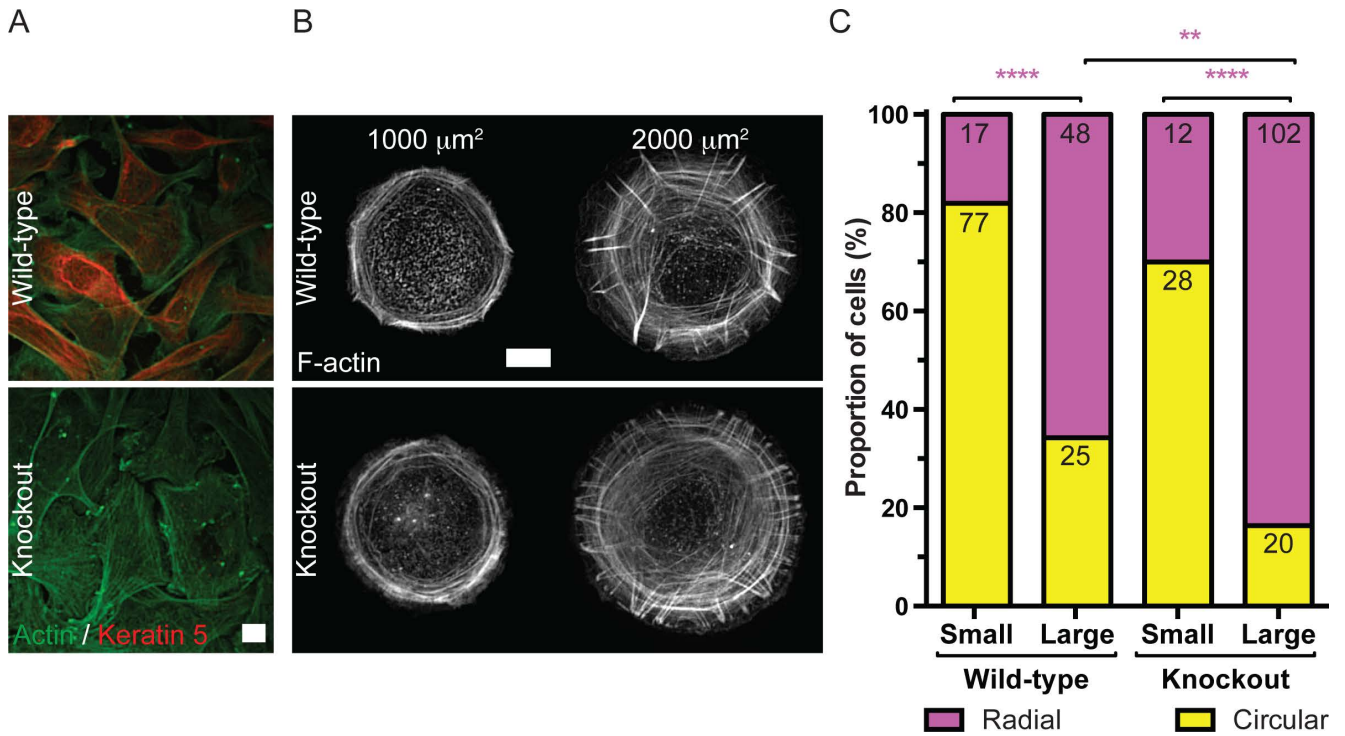


**Figure S8: Comparison of actin cytoskeleton self-organization between wild-type and keratin-null murine keratinocytes**

**A)** Representative images showing Actin ( $\beta$ -actin immunostaining) and Keratin5 (cytokeratin5 immunostaining) distribution in murine keratinocytes with normal (Wild-type) or depleted (Knockout) cytokeratin expression fixed after seeding on collagen-coated coverslips. Note Keratin5 staining was absent in Knockout cells. Scale bar: 10  $\mu$ m.

**B)** Representative images showing actin patterns in murine keratinocytes with normal (Wild-type) or depleted (Knockout) cytokeratin expression. Images show F-actin distribution (phalloidin staining) 24 h after seeding on collagen-coated islands of different sizes. Scale bar: 10  $\mu$ m.

**C)** Bar chart showing fractions of cells with actin cytoskeleton demonstrating circular or radial pattern from Wild-type or Knockout murine keratinocytes plated on Small (500, 750, 1000  $\mu$ m<sup>2</sup>) or Large (1500, 2000, 2500  $\mu$ m<sup>2</sup>) collagen-coated adhesive islands. Numbers of cells displaying each actin pattern are labelled on top of each bar, pooled from 3 and 2 independent experiments for Wild-type and Knockout cells respectively. Fisher's exact tests were used to assess significance between the fractions of cells displaying radial actin pattern in pairs (Wild-type on Small vs. Wild-type on Large, Wild-type on Small vs. Knockout on Small, Wild-type on Large vs. Knockout on Large, Knockout on Small vs. Knockout on Large); \* $P$ <0.05, \*\* $P$ <0.01, \*\*\* $P$ <0.001, \*\*\*\* $P$ <0.0001.



### Supplemental Tables

**Table S1: Non-keratinocyte epithelial cell spreading capacity on adhesive islands**

Table showing the number of cells under conditions shown in Fig. 2 that filled the circular shape when seeded on adhesive islands of different sizes (500, 750, 1000, 1500, 2000, 2500  $\mu\text{m}^2$ ). The number of cells selected after examination of 4, 3 and 2 dishes for MCF-10A, MCF-7 and NBT-II respectively are indicated.

Cell line	MCF-10A	MCF-7	NBT-II
<b>Number of independent experiments</b>	4	3	2
Projected cell area ( $\mu\text{m}^2$ )	Number of cells filling adhesive islands		
<b>500</b>	34	12	15
<b>750</b>	9	9	8
<b>1000</b>	5	4	10
<b>1500</b>	0*	1	5
<b>2000</b>	0	0	1
<b>2500</b>	0	0	1

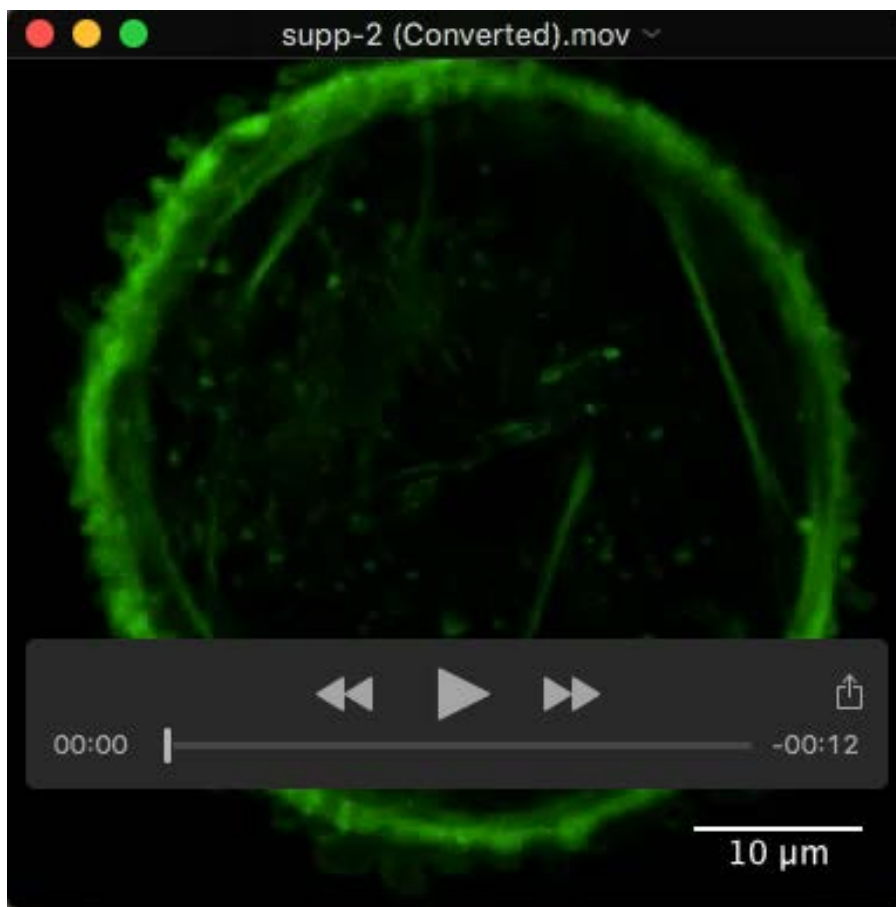
\*no cells filled adhesive islands of this size

**Table S2: Ovarian cancer cell lines spreading capacity on adhesive islands**

Table showing the number of cells under conditions shown in Fig. S4C that filled the circular shape when seeded on fibronectin-coated adhesive islands of different sizes (500, 750, 1000, 1500, 2000, 2500  $\mu\text{m}^2$ ).

Cell line	PEO1	OVCA429	SKOV3	HEYA8
Projected cell area ( $\mu\text{m}^2$ )	Number of cells filling adhesive islands			
<b>500</b>	23	16	3	3
<b>750</b>	11	8	10	7
<b>1000</b>	4	18	13	13
<b>1500</b>	0*	11	18	12
<b>2000</b>	2	13	19	15
<b>2500</b>	0	2	10	12

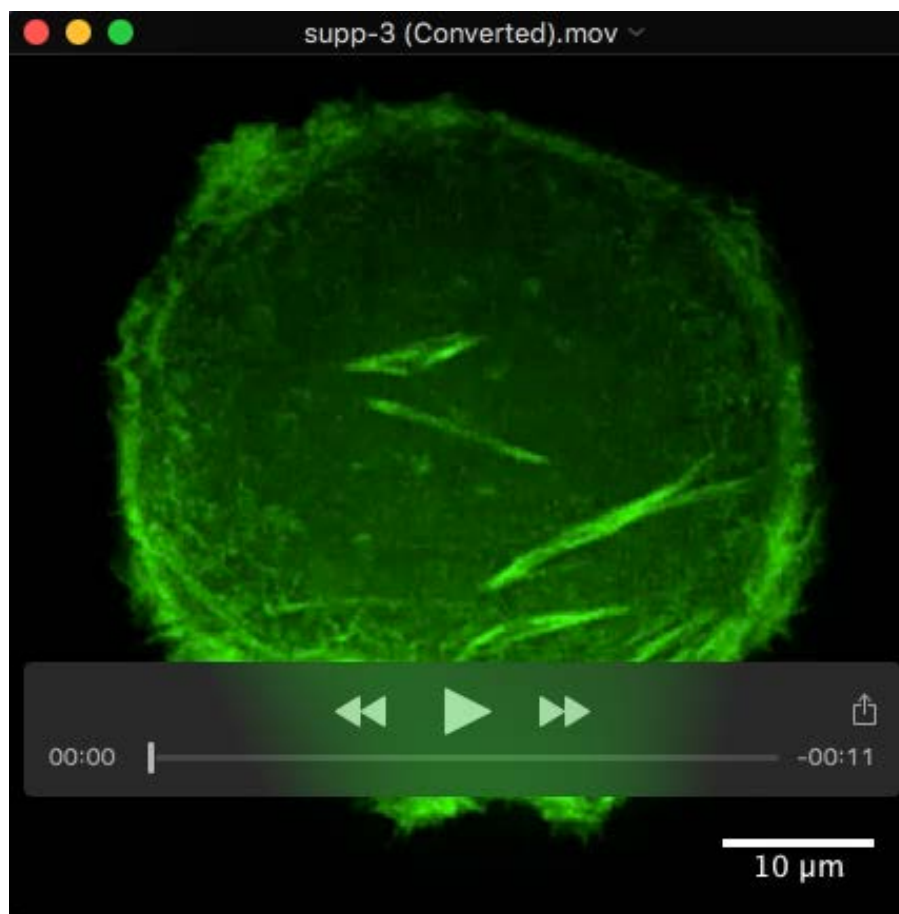
\*no cells filled adhesive islands of this size



***Movie 1: Evolution of actin cytoskeleton self-organization in fibroblasts***

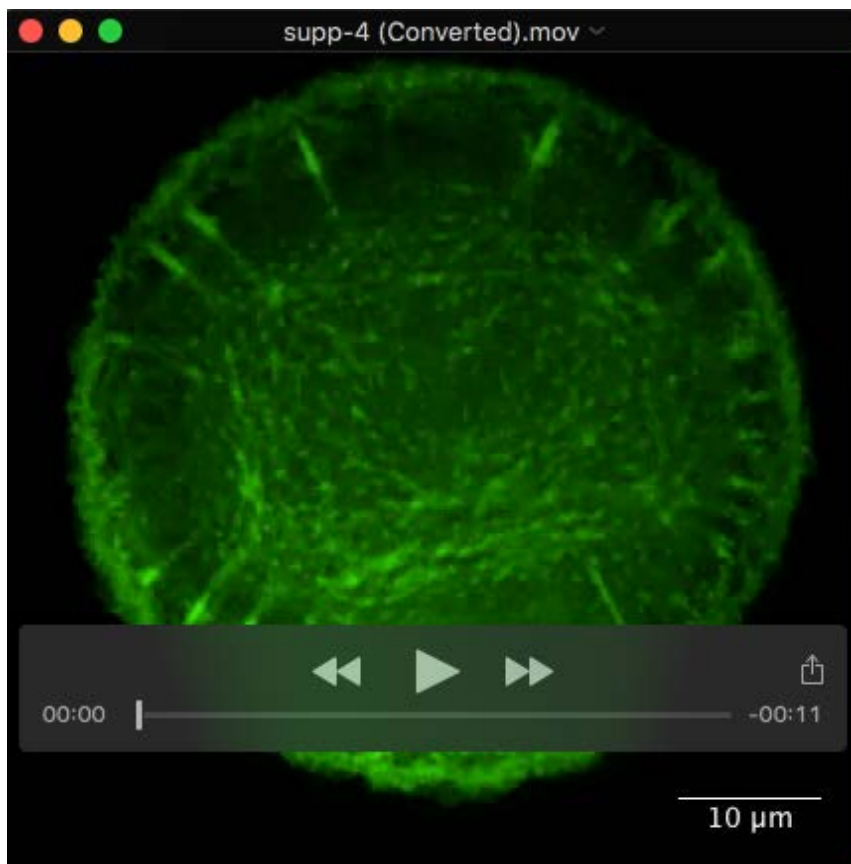
Representative time-lapse series showing actin cytoskeleton development in HFF cells expressing Lifeact-GFP plated on an  $1800 \mu\text{m}^2$  adhesive fibronectin-coated island. Note ventral stress fibres from first frame remain stable for first hour of movie.

Scale bar:  $10 \mu\text{m}$ . Timestamp: hh:mm. Playback rate:  $10 \text{ frames sec}^{-1}$ .



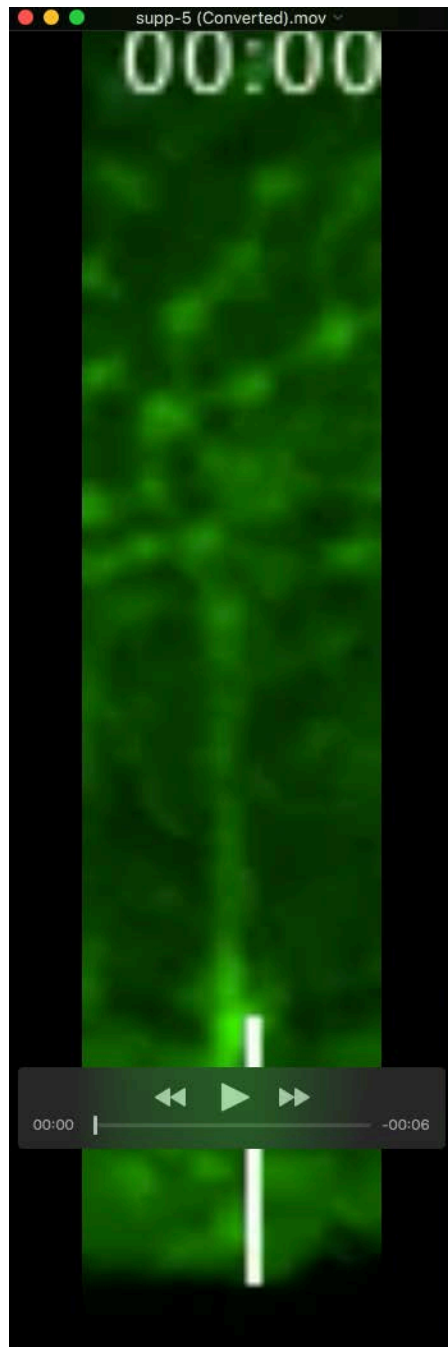
***Movie 2: Evolution of actin cytoskeleton self-organization in non-keratinocyte epithelial cells***

Representative time-lapse series showing actin cytoskeleton development in NBT-II cells expressing Lifeact-GFP plated on an 1800  $\mu\text{m}^2$  adhesive fibronectin-coated island. Note appearance of new short ventral stress fibres in the bottom half of cell over the first hour of movie. Scale bar: 10  $\mu\text{m}$ . Timestamp: hh:mm. Playback rate: 20 frames  $\text{sec}^{-1}$ .



***Movie 3: Evolution of actin cytoskeleton self-organization in non-keratinocyte epithelial cells after epithelial-mesenchymal transition***

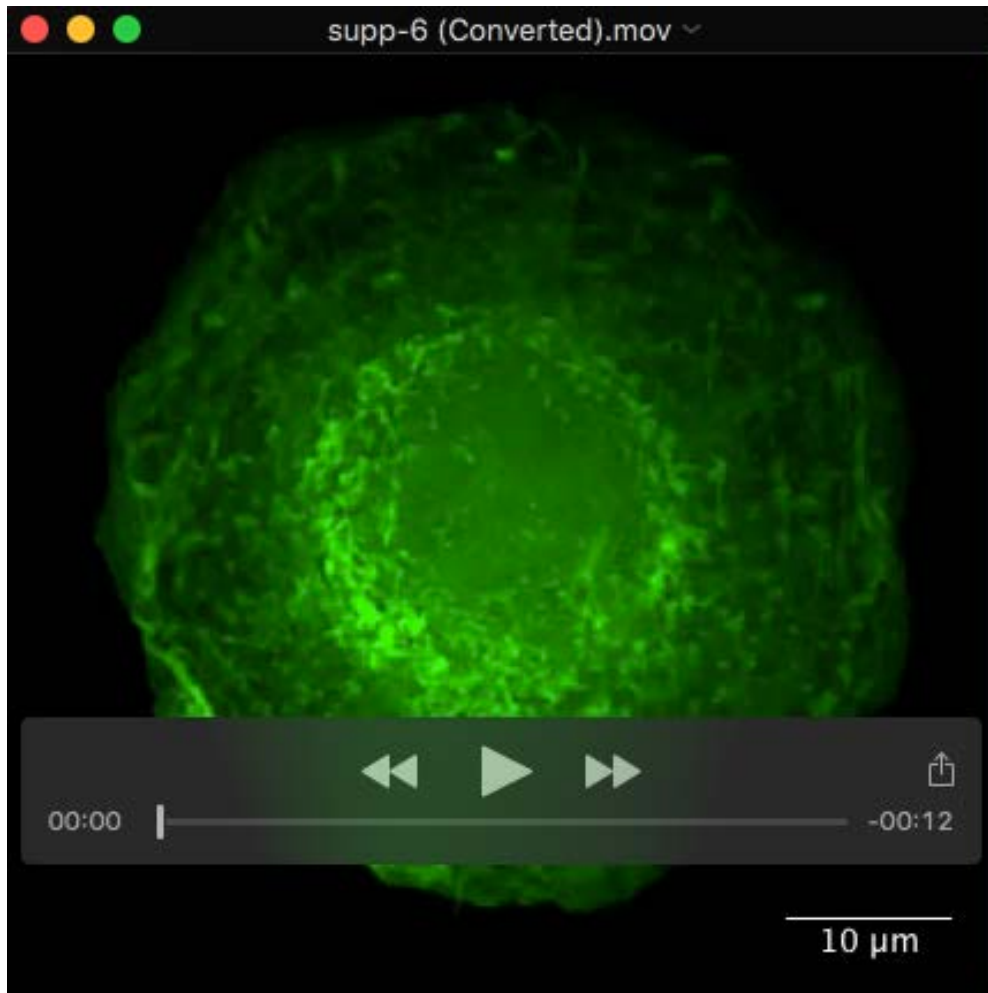
Representative time-lapse series showing actin cytoskeleton development in NBT-II cells expressing Lifeact-GFP pretreated with 100 ng ml<sup>-1</sup> Epidermal Growth Factor (EGF) for 3 days and replated on 1800 μm<sup>2</sup> fibronectin-coated islands in the continued presence of EGF. Scale bar: 10 μm. Timestamp: hh:mm. Playback rate: 20 frames sec<sup>-1</sup>.



***Movie 4: Centripetal directed movement of polygonal actin networks in EGF treated NBT-II cells***

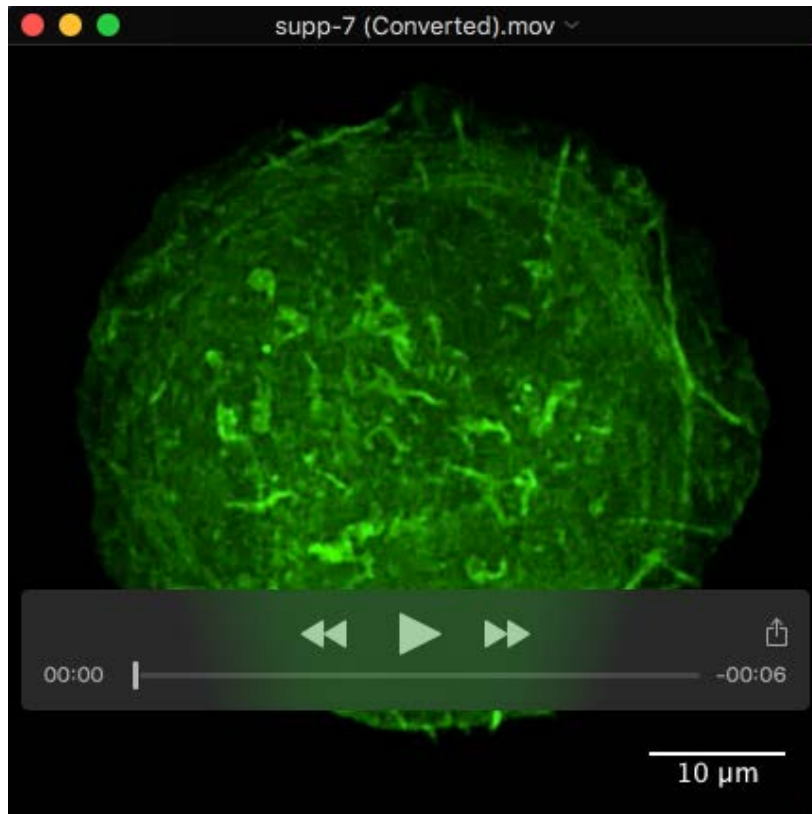
One hour long time-lapse showing region of actin cytoskeleton development in NBT-II cells expressing Lifeact-GFP pretreated with 100 ng ml<sup>-1</sup> Epidermal Growth Factor (EGF) for 3 days and replated on 1800  $\mu\text{m}^2$  fibronectin-coated islands in the continued presence of EGF, taken from region highlighted by a white box shown in the first frame of the EGF treated cell from Fig. 3A. Scale bar: 5  $\mu\text{m}$ . Timestamp: hh:mm. Playback rate: 5 frames sec<sup>-1</sup>.





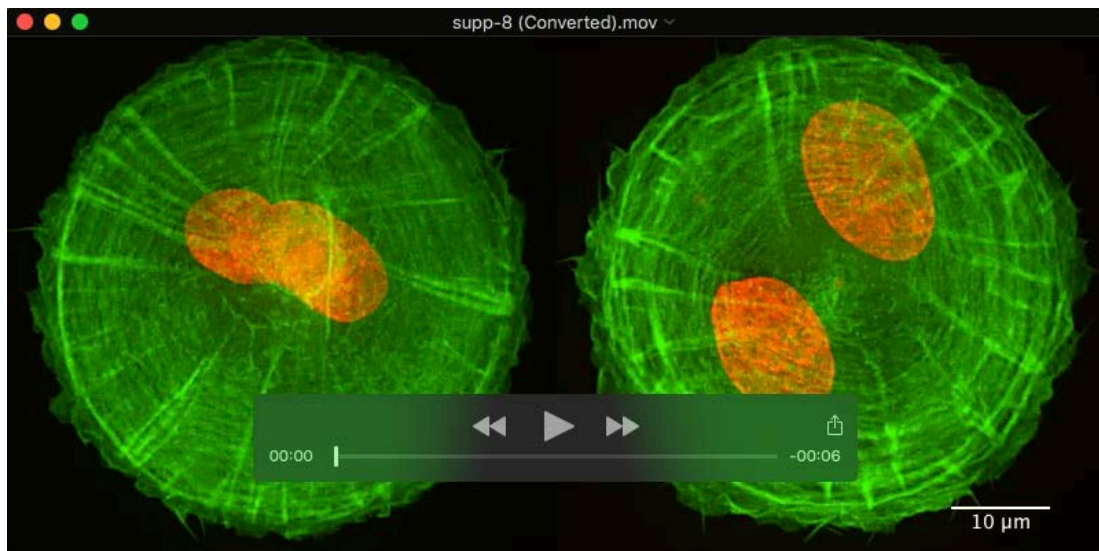
***Movie 5: Evolution of actin cytoskeleton self-organization in keratinocytes***

Representative time-lapse series showing actin cytoskeleton development in HaCaT cells expressing Lifeact-GFP plated on an 1800  $\mu\text{m}^2$  adhesive fibronectin-coated island. Scale bar: 10  $\mu\text{m}$ . Timestamp: hh:mm. Playback rate: 10 frames  $\text{sec}^{-1}$ .



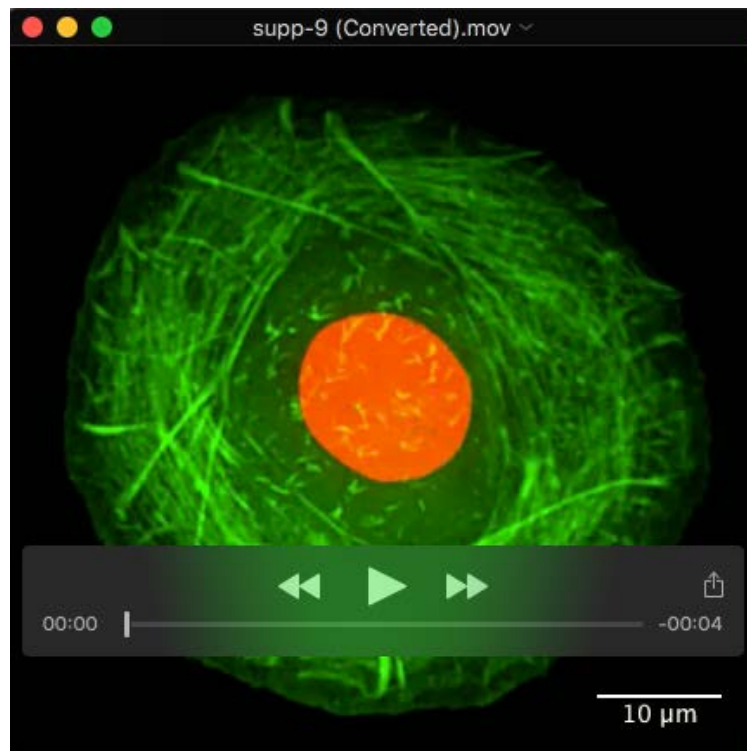
***Movie 6: Induction of chiral actin pattern development in keratinocytes***

Representative time-lapse series showing actin cytoskeleton development in HaCaT cells expressing Lifeact-GFP plated on an  $1800 \mu\text{m}^2$  adhesive fibronectin-coated island treated with 20 nM latrunculin A. Latrunculin A was added to cells 8 h after seeding. Scale bar:  $10 \mu\text{m}$ . Timestamp: hh:mm. Playback rate:  $10 \text{ frames sec}^{-1}$ .



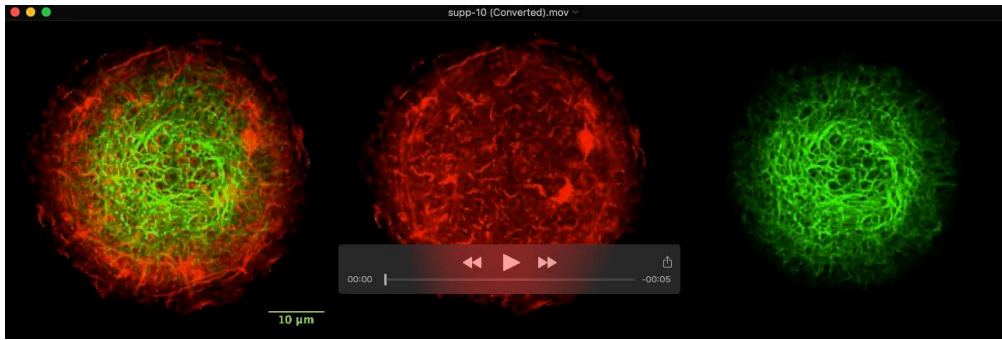
**Movie 7:**

Representative time-lapse series showing actin cytoskeleton development and nucleus rotation in diploid (left, untreated cells) or tetraploid (right, achieved by pre-treatment with cytochalasin D) HFF cells expressing GFP-Lifeact with BFP-NLS seeded on an  $1800 \mu\text{m}^2$  fibronectin-coated island. Scale bar:  $10 \mu\text{m}$ . Timestamp: hh:mm. Playback rate:  $10 \text{ frames sec}^{-1}$ .



***Movie 8: Rotation of the nucleus in latrunculin A-treated keratinocytes***

Representative time-lapse series showing actin cytoskeleton development and nucleus rotation in latrunculin A-treated HaCaT cells expressing GFP-Lifeact with RFP-H1 seeded on a 2000  $\mu\text{m}^2$  fibronectin-coated island. 200 nM of latrunculin A was added to cells 40 minutes after seeding. Scale bar: 10  $\mu\text{m}$ . Timestamp: hh:mm. Playback rate: 10 frames  $\text{sec}^{-1}$ .



***Movie 9: Evolution of actin and keratin cytoskeleton self-organization in keratinocytes***

Representative time-lapse series showing actin and keratin cytoskeleton development in HaCaT cells expressing mRuby-Lifeact and mEmerald-Keratin14 plated on an 1800  $\mu\text{m}^2$  adhesive fibronectin-coated island. Scale bar: 10  $\mu\text{m}$ . Timestamp: hh:mm. Playback rate: 10 frames  $\text{sec}^{-1}$ .





***Movie 10: Evolution of actin and keratin cytoskeleton self-organization in keratinocytes in the chiral actin pattern***

Representative time-lapse series showing cytoskeleton progression in latrunculin A-treated HaCaT cells expressing mEmerald-Keratin14 with mRuby-Lifeact seeded on  $1800 \mu\text{m}^2$  fibronectin-coated islands. 20 nM of latrunculin A was added to cells 8 h after seeding. Scale bar:  $10 \mu\text{m}$ . Timestamp: hh:mm. Playback rate:  $10 \text{ frames sec}^{-1}$ .